Ordered Polyelectrolyte "Multilayers". 6. Effect of Molecular Parameters on the Formation of Hybrid Multilayers Based on Poly(Diallylammonium) Salts and Exfoliated Clay

P. Y. Vuillaume,[†,§] K. Glinel,[‡,||] A. M. Jonas,[‡] and A. Laschewsky*[,†]

Département de Chimie, Université Catholique de Louvain, Place L. Pasteur, 1, B-1348 Louvain-la-Neuve, Belgium, and Unité de Physique et de Chimie des Hauts Polymères, Université Catholique de Louvain, Place Croix du Sud, 1, B-1348 Louvain-la-Neuve, Belgium

Received October 22, 2002. Revised Manuscript Received June 12, 2003

A new series of poly(diallylammonium) salts with varying hydrophilic−hydrophobic balance and bulkiness was prepared, to investigate the impact of these parameters on the formation of electrostatic layer-by-layer assemblies. The polycations were self-assembled on quartz and silicon substrates together with Laponite, a synthetic, negatively charged alumino-silicate clay. This system was found to be quite robust for forming lamellar heterostructures of controlled thickness at the solid interfaces. Bulky and hydrophobic, as well as amphiphilic, polycations can be accommodated between the rigid exfoliated aluminosilicate platelets without disrupting the lamellar-like structure. Ellipsometry and X-ray reflectivity showed that substituents attached to the backbone have a significant impact on both the growth process and the extent of the ordered region. Hydrophobicity and bulkiness favored the formation of thicker films, presumably due to the more coily conformation of the polycation during the deposition. Films are only partially organized and coherence lengths along the normal of the plane are in the range 2.7−7.5 nm. The values depend sensitively on the detailed chemical structure of the polyelectrolyte employed and the nature of the solvent used for the deposition process.

Introduction

The extensive use of the versatile electrostatic self-assembly technique (ESA) for forming layer-by-layer thin films has enriched the understanding of ordering of polyelectrolytes at solid interfaces.[1] Nevertheless, little progress has been made so far concerning the fabrication of ordered polyelectrolyte multilayer assemblies. Although one recent paper demonstrates that it is possible to obtain ordered assemblies—i.e., with well-defined stratas that we define as layers of homogeneous composition—by complexing certain cationic ionenes with common polyanions,[2] there is a consensus that such ordering is rather exceptional for most binary polyelectrolyte systems. Indeed, specific Coulombic interactions tend to compatibilize on a very short length scale (probably at the molecular level) the two complementary polyelectrolytes through a diffusion process that occurs at the interface.[2] On one hand, gradual transition of physical properties at interfaces may serve a number of applications.[3] On the other hand, e.g. for a number of optical[4] and electronic devices,[5] a well-defined modulation of both chemical composition and structural properties in a direction normal to the substrate is desirable. Recently, improved structural ordering of ultrathin films was reported by self-assembling polyelectrolytes and inorganic platelets.[6,7] This procedure, which simply extends the procedure developed by Decher and co-workers,[8] consists of the sequential adsorption of two heterospecies, namely the polyelectrolyte and the two-dimensional inorganics nanoplate-

* To whom correspondence should be addressed at new affiliation: Fraunhofer Institut für Angewandte Polymerforschung FhG-IAP; Geiselbergstrasse 69; D-14476 Golm, Germany. Phone: +49-331-568-1327. Fax: +49-331-568-3000. E-mail: andre.laschewsky@iap.fhg.de.

† Département de Chimie, Université Catholique de Louvain.

‡ Unité de Physique et de Chimie des Hauts Polymères, Université Catholique de Louvain.

§ New address: Université de Montréal, Faculté de Médecine Vétérinaire, Département de Virologie, 3200 rue Sicotte Saint-Hyacinthe, Québec J2S 2M2, Canada

|| New address: UMR 6522 "Polymères, Biopolymères, Membranes", CNRS −Université de Rouen, Bd Maurice de Broglie, F-76 821 Mont-Saint-Aignan, France.

(1) See review articles: (a) Bertrand, P.; Jonas, A.; Laschewsky, A.; Legras, R. *Macromol. Rapid Commun.* **2000**, *21*, 319. (b) Arys, X.; Jonas, A. M.; Laschewsky, A.; Legras, R. In *Supramolecular Polymers*; Cifferi, A., Ed.; Marcel Dekker: New York, 2000; p 505.

(2) (a) Arys, X.; Laschewsky, A.; Jonas, A. M. *Macromolecules* **2001**, *34*, 3318. (b) Arys, X.; Fischer, P.; Jonas, A. M.; Koetse, M. M.; Laschewsky, A.; Legras, R.; Wischerhoff, E. *J. Am. Chem. Soc.* **2003**, *125*, 1859.

(3) Li, D. Q.; Lütt, M., Fitzsimmons, R.; Synowicki, R.; Hawley, M. E.; Brown, G. W. *J. Am. Chem. Soc.* **1998**, *120*, 8797.

(4) (a) Ungashe, S. B.; Wilson, W. L.; Katz, H. E.; Scheller, G. R. *J. Am. Chem. Soc.* **1992**, *114*, 8717. (b) Li, D.; Ratner, M. A.; Marks, T.; Zhang, C. H.; Yang, J.; Wong, G. K. *J. Am. Chem. Soc.* **1990**, *112*, 7389.

(5) Byrd, H.; Suponeva, E. P.; Bocarsly, A. B.; Thompson, M. E. *Nature* **1996**, *380*, 610.

(6) (a) Kleinfeld, E. R.; Fergusson, G. S. *Science* **1994**, *265*, 370. (b) Kleinfeld, E. R.; Fergusson, G. S. *Chem. Mater.* **1995**, *7*, 2327. (c) Kleinfeld, E. R.; Fergusson, G. S. *Chem. Mater.* **1996**, *8*, 1575.

(7) Glinel, K.; Jonas, A. M.; Laschewsky, A.; Vuillaume, P. Y. Strategies to Internally Structured Polyelectrolyte Multilayers. In *Thin Films: Polyelectrolyte Multilayers and Related Multicomposites*; Decher, G., Schlenoff, J., Eds.; Wiley-VCH: Weinheim, 2003; pp 177−205.

10.1021/cm021338q CCC: $25.00
Published on Web 08/12/2003

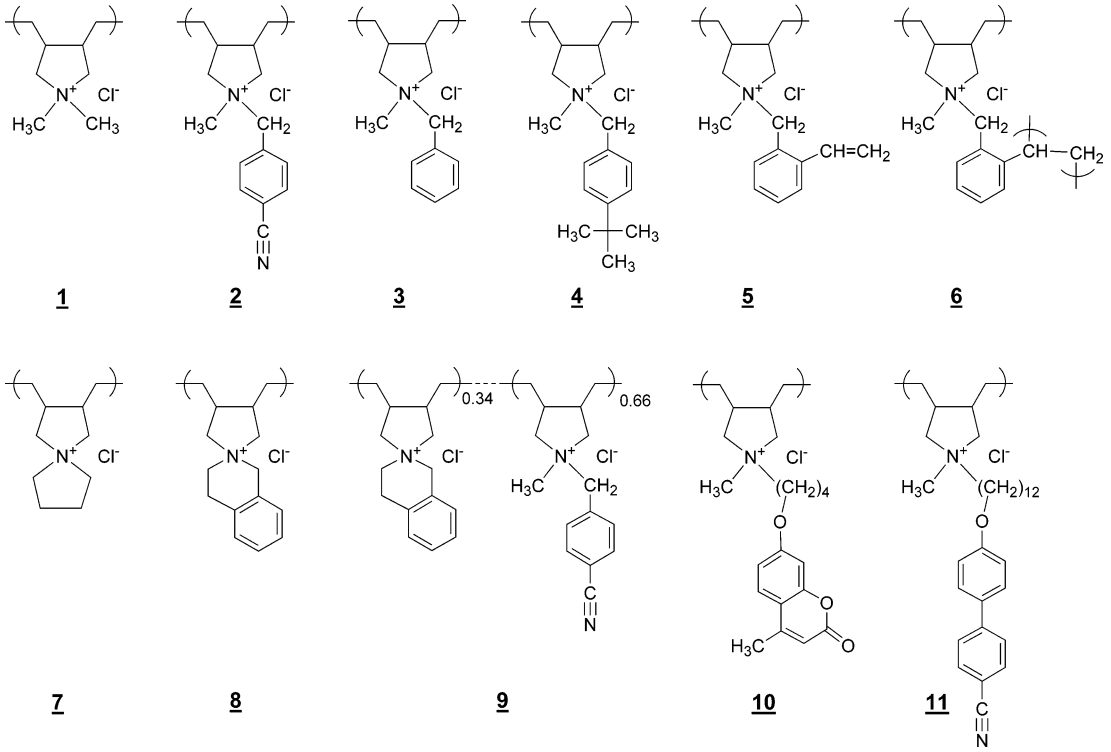

Figure 1. Poly(diallylammonium) salts used as organic counter-polycations of negatively charged Laponite platelets for the preparation of $\{\mathbf{A},\mathbf{L}\}_n$ hybrid multilayers.

lets which can be obtained by exfoliation of charged inorganic materials, such as layered alumino-silicate clays.

The morphology of these nanosheets seems appropriate to stabilize and induce structure in the stratified assemblies: due to the anisotropy of shape, the high surface area, and the rigidity of the platelets, tiling might be expected to occur in a regular fashion by covering the surface of the adsorbed flexible complementary polyelectrolyte, rather than diffusing into the polyelectrolyte films. So far, the best documented ESA hybrid systems are made from the strong polyelectrolyte poly(diallyldimethylammonium) salt (PDADMAC, **1**), combined with various smectite clays such as montmorillonite[9] and Laponite (**L**),[6,10−11] a synthetic clay of the group of hectorites. In these systems, the straightforward evidence of ordering is provided by the presence of Bragg peaks in the X-ray reflectograms.[10] However, it was demonstrated that true layering of the silicate platelets only occurs close to the substrate, while platelets further away are staggered randomly to produce a structure closer to a nanocomposite with preferential alignment of platelets than to a true multilayer.[9,11] Similar results were obtained for other families of polycations such as polymethacrylates and ionenes.[10] Among the investigated systems, poly(diallylammonium) salt derivatives appeared as attractive candidates because the order in such multilayers subsides over longer distances from the substrate, although limited to only about 60 Å.[10] For most internally ordered systems studied to date,[6−7,9−12] the increment of thickness per dipping cycle was usually found to be different from the internal repeat period, by a factor of 0.3 to 2. This was explained by considering that ordering happens upon complexation between the polyions in a water-swollen region at the surface of the film. This complexation involves significant rearrangements of the previously adsorbed "layer", therefore decorrelating the values of repeat period from the increments of thickness per adsorption cycle.

In another variation of the molecular structures explored, a cross-linkable unsaturated polydiallylammonium was recently employed in an attempt to stabilize hybrid heterostructures via photo-cross-linking.[12] Except for this attempt and one of our previous works,[10] relatively little effort has been yet devoted to investigating the effect of varying the details of the molecular structures on the growth and structuring process. In this paper, we study this aspect by establishing some relationships between the differences observed in structure formation with the variations imposed to the molecular structure of the polycations, namely by investigating the different poly(diallylammonium) salts presented in Figure 1. These polycations can be categorized into several groups according to their solubility

(8) (a) Decher, G. *Science* **1997**, *277*, 1232. (b) Decher, G. In *The Polymer Materials Encyclopedia: Synthesis, Properties and Applications*; Salamone, J. C., Ed.; CRC Press: Boca Raton, FL, 1996; pp 4540−4546. (c) Decher, G. *Comprehensive Supramolecular Chemistry (Templating, Self-Assembly and Self-Organization)*; Oxford, 1996; vol. 9, p 507.

(9) (a) Kotov, N. A.; Haraszti, T.; Turi, L.; Zaval, G.; Geer, R. E.; Dékány, I.; Fendler, J. H. *J. Am. Chem. Soc.* **1997**, *119*, 6821. (b) Mamedov, A. A.; Ostrander, J.; Aliev, F.; Kotov, N. A. *Langmuir* **2000**, *16*, 3941. (c) Mamedov, A. A.; Kotov, N. A. *Langmuir* **2000**, *16*, 5530. (d) Malikova, N.; Pastoriza-Santos, I.; Schierhorn, M.; Kotov, N. A.; Liz-Marzán, L. M. *Langmuir* **2002**, *18*, 3694. (e) Fan, X. W.; Locklin, J.; York, J. H.; Blanton, W.; Xia, C. J.; Advincula, R. *Chem. Mater.* **2002**, *14*, 2184.

(10) Glinel, K.; Laschewsky, A.; Jonas, A. M. *Macromolecules* **2001**, *34*, 5267.

(11) Glinel, K.; Laschewsky, A.; Jonas, A . M. *J. Phys. Chem. B.* **2002**, *106*, 11246.

(12) Vuillaume, P. Y.; Jonas, A. M.; Laschewsky, A. *Macromolecules* **2002**, *35*, 5004.

and the targeted physical applications. Poly(diallylammonium) salts **1**, **2**, **3**, and **4** were designed with respect to the variation of their hydrophilic−hydrophobic balance; polycations **1**, **7**, and **8** were designed with respect to the variation of their bulkiness and rigidity; and functional polycations **5**, **10**, and **11** were considered for their potential interest in cross-linking,[12] photophysical,[13] and structural studies. ESA assemblies will be presented under the form $\{\mathbf{A},\mathbf{L}\}_n$, describing a multilayer film made of *n* cycles of polycation **A** with the inorganic polyanion Laponite, **L**.

Experimental Section

Materials. 4-Bromomethylbenzonitrile, [Aldrich, (99%)], benzyl chloride [Aldrich, (99%)], (4-*tert*-butyl)benzyl chloride [Aldrich, (99%)], 2,2′-dimethyl-2,2′-azo-*N*-(2-hydroxyethyl)propionamide [VA086, gift from WAKO] were used as received. All solvents used were analytical grade. Acetonitrile (Merck) was dried over molecular sieves (4 Å). Potassium persulfate ($K_2S_2O_8$, Acros) was crystallized from water. The anion exchange of ammonium bromides to the chlorides employed an exchange resin (IRA-400, Fluka) loaded with Cl^-. Thin-layer chromatography (TLC) was carried out on precoated silica gel (Kieselgel 60, Merck, F-254) or on alumina (aluminum oxide Kieselgel 60-F254). Water used for the dialysis and the rinse solution for multilayer fabrication was purified by an Elgastat maxima purification system (resistance 18.2 MΩ·cm).

Synthesis and characterization of the bulky polycation **8** as well as its conversion to a cross-linkable polycation **5**, that could be cross-linked leading to the polycation **6**, were described in a previous communication.[12] The preparation of monomers and polymers **10** and **11** bearing fluorescent and mesogenic groups will be detailed elsewhere.[13] Laponite [elementary analysis (%): SiO_2, 60; MgO, 29; Li_2O, 0.9; Na_2O, 2,9; 9.8 weight loss by ignition] from Laporte Industry was a gift from Chimilab Essor (La Madeleine, France).

Preparation of the Multilayered Assemblies. Two different substrates were used. Quartz plates (Suprasil) and silicon wafers (100) were cleaned for 1 h in a piranha mixture [H_2SO_4/H_2O_2 (30%) 1:1 (v/v)] (*Caution: "piranha solution" is extremely corrosive and reacts violently with organic compounds*), and then abundantly rinsed with ultrapure water before use. No buffer layer was deposited as first precoated monolayer. Syringe filters (PTFE) of a porosity of 0.45 μm served for filtering polyelectrolyte solutions (10^{-2}−10^{-3} mol·L^{-1}) and Laponite dispersions (concentration 0.25 wt %). The deposition process was carried out in two steps corresponding to one dipping cycle. First, the clean substrate was immersed into an aqueous solution containing the polycation, except for the polycations **4**, **5**, **10**, and **11** that were found insoluble in pure water. DMSO was used for **5** and **6** (see ref 12 for more details); a water/ethanol mixture (50/50 v/v) was used for **4** and **10**, and $CHCl_3$ was employed for **11**. Second, after drying of the deposited layer in a warm stream of air, the film was immersed into a water-based dispersion of the exfoliated Laponite, rinsed, and dried. The process was cycled with the aid of a robotized system (Kirstein and Riegler, Berlin, Germany) to produce multilayers.

Techniques. (a) NMR spectra were recorded at ambient temperature on Varian Gemini 200 and 300 MHz spectrometers. Chemical shifts, δ, are given in ppm with respect to the solvent residual resonances fixed at 7.27, 4.80, and 3.30 ppm for $CDCl_3$, D_2O, and CD_3OD, respectively. (b) Elemental analysis (C, H, N, Cl) was performed at the University College London (Chemistry Department). (c) Mass spectra were run using a SCIEX API III triple quadruple mass spectrometer (Mass Spectrometry Lab, Université Catholique de Louvain). (d) Infrared spectra of samples ground in KBr pellets were recorded on a Bruker Equinox FTIR spectrometer. The chamber was flushed for 15 min with dried air before each measurement. A total of 256 scans at a resolution of 2 cm^{-1} were averaged. (e) UV/Vis absorption spectra were obtained on a Varian Carry SE spectrometer from films deposited on clean quartz plates. Maxima observed in the first derivative of the absorbance spectra were obtained after smoothing the data by the Savitsky Golay algorithm. (f) Thermogravimetric analysis was carried out under constant nitrogen flow (200 mL·min^{-1}) at a heating rate of 10 °C/min using a Mettler Toledo STAR^e system. The samples were previously dried in situ at 80 °C for 15 min just prior to the heating scans. The first derivatives of the scans were used to determine the main weight loss. (g) Ellipsometry measurements were run on a Digisel rotating compensator ellipsometer (Jobin-Yvon/Sofie Instruments), at the wavelength of 6328 Å (He−Ne laser) and a fixed incidence angle of 70°. Each data point was averaged by performing two measurements with the analyzer successively set to +45° and −45° (with respect to the plane of incidence). Procedure details are given elsewhere.[2,10] For each sample, the given thickness is the average result of at least six different measurements made at different positions. A refractive index of 1.47 was used for the data treatment. The native oxide layer atop the silicon substrate leads to an overestimation of the film thickness by about 15 Å. (h) The X-ray reflectometry (XRR) measurements were carried out on a Siemens D 5000 2-circles goniometer using Cu Kα radiation (λ = 1.5418 Å) from a rotating anode operating at 40 kV and 300 mA; wavelength selection was achieved by way of a graphite secondary monochromator and pulse height discrimination (proportional counter). Collimation was effected by slits adjustable with micrometer precision. Additional information on the experimental setup can be found elsewhere.[14] Intensities are reported as a function of K_{z_0}, the component perpendicular to the interface of the wavevector in the vacuum of the incident photons [i.e., $K_{z_0} = (2\pi/\lambda)\cdot\sin\theta$, where λ is the X-ray wavelength and θ is half the scattering angle]. To determine the position of the Bragg peaks, intensities were multiplied by $K_{z_0}^4$ and plotted versus K_{z_0}. Organic sublayers thicknesses, *p*, were calculated from the basal spacing, *d*, by assuming that the thickness occupied by each inorganic layer is 9.2 Å ($p = d - 9.2$).[15] Patterson functions were obtained by Fourier transformation as described elsewhere.[2] Coherence lengths in the direction normal to the substrate surface were also obtained by fitting an exponential function [$\exp(-z/\xi)$] passing through the subsidiary maxima of the Patterson functions. The coherence length was defined as $L_{coh} = 3\xi$ (Table 1) which represents approximately the largest distance over which correlation subsides between sublayers. The thicknesses of the films were determined from the Kiessig fringes in the reflectogram (when any), or, equivalently, from the position of the final correlation peak of the Patterson functions.

Synthesis of Monomers. *N,N-Diallyl-N-methyl-(4-benzonitrile)ammonium chloride,* ***m2***. Under a dry argon atmosphere, 6.05 g (0.031 mol) of bromomethylbenzonitrile and 5.42 g of diallylmethylamine (0.048 mol) that was synthesized according to ref.[16] were dissolved in 35 mL of acetonitrile and refluxed for 2 days. The solution was concentrated and then precipitated in cold ether. The crude viscous oil was dissolved in 20 mL of water and washed three times with ether (50 mL). Pure product was recovered by freeze-drying and dried overnight in vacuo at 40 °C. Yield: 9.11 g (62%) in the form of a viscous oil. *N,N*-diallyl-*N*-methyl-4-benzonitrile ammonium bromide (9.1 g, 0.032 mol) was dissolved in water and an equimolar amount of Cl^- loaded anion-exchange resin was added. The mixture was stirred for 20 min before the resin was filtered off. The same procedure was carried out a second time and the resulting aqueous solution was lyophilized to give

(13) Habib-Jiwan, J. L.; Laschewsky, A.; Moussa, A.; Rullens, F.; Vuillaume, P. Y. to be submitted for publication.

(14) Bollinne, C.; Stone, V. W.; Carlier, V.; Jonas, A. M. *Macromolecules* **1999**, *32*, 4719.

(15) (a) Ramsay, J. D. F. *J. Colloid Interface Sci.* **1986**, *109*, 441. (b) Ramsay, J. D. F.; Linder, P. J. *Chem. Soc., Faraday Trans.* **1993**, *89*, 4207.

(16) Favresse, P.; Laschewsky, A. *Macromol. Chem. Phys.* **1999**, *200*, 887.

Table 1. Data of The $\{A,L\}_n$ Multilayers Obtained from Ellipsometry, X-ray Reflectivity, and Computed Patterson Functions

$\{A,L\}_n$	solvent for polycation	total film thickness[a] (Å)	thickness increment per cycle[b] (Å/cycle) (±1 Å)	*d*, Bragg distance[c] (Å) (±0.5 Å)	p^d (Å)	ratio R^e	L_{coh}[f,g] (Å)	total film thickness[g] (Å)
$\{\mathbf{1},\mathbf{L}\}_{16}$	H_2O		17[i]	14.4[i]	5.2[i]	1.2[i]	66	
$\{\mathbf{2},\mathbf{L}\}_{15}$	H_2O	315[h]	21	14.8	5.6	1.4	60	395
$\{\mathbf{3},\mathbf{L}\}_{15}$	H_2O	389	26	14.3	5.1	1.8	63	361
$\{\mathbf{4},\mathbf{L}\}_{15}$	H_2O/EtOH	522	31	19.6	10.4	1.5	33	397
$\{\mathbf{5},\mathbf{L}\}_{15}$	DMSO		19[j]	15.8[j]	6.6[j]	1.2[j]	36	
$\{\mathbf{6},\mathbf{L}\}_{15}$	DMSO		5[j]	15.9[j]	6.7[j]	0.3[j]	31	
$\{\mathbf{7},\mathbf{L}\}_{16}$	H_2O		21[i]	14.4[i]	5.2[i]	1.5[i]	60	
$\{\mathbf{8},\mathbf{L}\}_{15}$	H_2O	494	32	15.5	6.3	2.1	51	487
$\{\mathbf{9},\mathbf{L}\}_{15}$	H_2O	483	31	15.3	6.1	2.0	63	499
$\{\mathbf{10},\mathbf{L}\}_{15}$	H_2O/EtOH	460	31	18.7	9.5	1.7	45	425
$\{\mathbf{11},\mathbf{L}\}_{16}$	$CHCl_3$	567	34	31.8/13.2	22.6	1.1	75	548

[a] From ellipsometry. [b] From regression curve of ellipsometric data. [c] From X-ray reflectometry. [d] Calculated thickness of the organic sublayer: $p = (d - 9.2$ Å). [e] *R* is the ratio of the thickness increment per adsorption cycle (according to ellipsometry) to the Bragg spacing (according to X-ray reflectometry). [f] Coherence length. [g] Obtained from the computed Patterson function. [h] Interpolated data. [i] Data taken from ref 10. [j]Data taken from ref 12.

6.53 g (83%) of a yellowish hygroscopic paste. Anal. Calcd for $C_{15}H_{19}N_2Cl{\cdot}H_2O$ ($M_r = 262.78 + 18.02$): C, 64.16; H, 7.54; N, 9.98; Cl, 12.63; C/N = 6.43. Found: C, 63.75; H, 7.29; N, 9.34; Cl, 11.19; C/N = 6.82. ^{1}H NMR (200 MHz, $CDCl_3$): δ = 8.10−7.50 [m, 4H, *aromatic H*]; 6.25−5.90 [m, 2H, >C=C*H*]; 5.80−5.50 [m, 4H, H_2C=C<]; 4.87 [s, 2H, ($^+$N)−CH_2−Φ], 4.2 [m, 4H, C=C−CH_2]; 3.13 [s, 3H, N−CH_3]. ^{13}C NMR (50 MHz, $CDCl_3$): δ = 135.0, 133.3, 130.5, 125.0, 124.7, 118.3, 115.1 [C_{Aryl} + CH_2 = *C*H− + *C*N]; 64.2 [(N^+)−CH_2−Φ + (N^+)−*C*H_2−C=]; 47.3 [(N^+)−*C*H_3]. MS(FAB): $m/z = (M - Cl^-)^+ = 227.2$.

N,N-Diallyl-N-methyl-benzylammonium Chloride, ***m3***. Under a dry argon atmosphere, 18.1 g (0.144 mol) of benzyl chloride and 8.0 g of diallylmethylamine (0.072 mol) were dissolved in 70 mL of acetonitrile and refluxed for 2 days. The solution was concentrated and then precipitated in cold ether. The crude viscous oil was dissolved in 20 mL of water and washed three times with 50 mL of diethyl ether. Pure product was recovered by lyophilization and dried overnight in vacuo at 40 °C. Yield: 16.2 g (87%) of a viscous oil. Anal. Calcd for $C_{14}H_{20}NCl{\cdot}H_2O$ ($M_r = 237.77 + 18.02$): C, 65.74; H, 8.67; N, 5.48; Cl, 13.86; C/N = 12.00. Found: C, 66.48; H, 8.67; N, 5.51; Cl, 14.16; C/N = 12.06; ^{1}H NMR (200 MHz, $CDCl_3$ + CD_3OD): δ = 7.60−7.10 [m, 5H, *aromatic H*]; 6.05−5.75 [m, 2H, >C=C*H*−]; 5.70−5.40 [m, 4H, H_2C=C−]; 4.76 [s, 2H, ($^+$N)−CH_2−Φ], 4.20−3.80 [m, 4H, C=C−CH_2]; 2.94 [s, 3H, ($^+$N)−CH_3]. ^{13}C NMR (50 MHz, $CDCl_3$): δ = 134.1, 131.9, 130.3, 130.0, 128.1, 125.5 [C_{Aryl} + CH_2=*C*H−]; 66.4, 64.4 [(N^+)−*C*H_2−Φ + (N^+)−*C*H_2−C=]; 47.4 [(N^+)−*C*H_3]. MS(FAB): $m/z = (M - Cl^-)^+$ = 202.1.

N,N-Diallyl-N-methyl-(4-tert-butyl)benzylammonium Chloride, ***m4***. Same procedure as for ***m3*** starting with 5.0 g (0.027 mol) of (4-*tert*-butyl)benzyl chloride and 4.6 g (0.041 mol) of diallylmethylamine. Yield 7.96 g (99%) of a viscous oil. Anal. Calcd for $C_{18}H_{28}NCl{\cdot}0.5\ H_2O$ ($M_r = 293.88 + 9.01$): C, 71.38; H, 9.65; N, 4.62; Cl, 11.70; C/N = 15.44. Found: C, 71.94; H, 10.02; N, 4.61; Cl, 10.50; C/N = 15.61. ^{1}H NMR (200 MHz, $CDCl_3$): δ = 7.60−7.30 [m, 4H, *aromatic H*]; 6.25−5.90 [m, 2H, >C=C*H*−]; 5.85−5.60 [m, 4H, H_2C=C−]; 4.88 [s, 2H, ($^+$N) − CH_2 − Φ], 4.35−4.00 [m, 4H, C=C−CH_2]; 3.13 [s, 3H, (N^+) − CH_3]; 1.28 [s, 9H, Φ−C−(CH_3)$_3$]. ^{13}C NMR (50 MHz, CD_3-OD): δ = 155.2, 134.2, 129.4, 127.4, 126.5, 125.9 [C_{Aryl} + $C_{allyl}H_2$=C + C=C_{allyl}H]; [CH_3−(N+), hidden by the CD_3OD signal]; 66.9, 64.8 [(N^+)−*C*H_2−Φ + (N^+)−*C*H_2−C=]; 35.9 [(CH_3)$_3$−*C*−Φ]; 31.8 [(*C*H_3)$_3$−C−Φ]. MS(FAB): $m/z = (M - Cl^-)^+ = 258.4$.

Polymerization. After at least three freeze−thaw cycles, monomers were polymerized in aqueous solution during 48 h with 4 mol/% of VA086 or $K_2S_2O_8$ at 60 or 70 °C, respectively. Polymers were purified by exhaustive (at least 3 days) dialysis using dialysis membranes (Spectra/Por) with a nominal cutoff of 6000−8000 Da. The polymers were recovered by freeze-drying and dried at 40 °C in vacuo.

Poly(N,N-diallyl-N-methyl-N-(4-cyanobenzyl)ammonium) Chloride, ***2***. White hygroscopic powder, ^{1}H NMR (200 MHz, CD_3OD): δ = 8.10−7.50 [2 signals, *aromatic H*]; 4.90−4.50 [broad, ($^+$N)−CH_2−Φ]; 4.25−2.10 [broad peaks, ($^+$N)−CH_3 + C−C−CH_2−(N^+)]; 1.90−0.90 [broad peaks, CH_2 backbone]. FT-IR [KBr, selected bands (cm^{-1})]: [3092, 3050, 3030, 3003, Ar−H]; [2938, 2867, CH, *ν* sym and antisym]; [2231;−CN, *ν*]; [1121, −O−SO_3^-]; [831, Ar−H, δ_{oop} o-disubstituted]; [624, −O−SO_3^-]; [557, Ar−H, o-disubstituted].

Poly(N,N-diallyl-N-methyl-N-(4-benzyl)ammonium) Chloride, ***3***. White hygroscopic powder. ^{1}H NMR (200 MHz, $CDCl_3$): δ = 7.75−7.25 [two signals, *Aromatic H*]; 4.80−4.20 [broad peaks, ($^+$N)−CH_2−Φ]; 4.20−2.10 [broad peaks, ($^+$N)−CH_3 + C−C−CH_2−(N^+)]; 1.80−0.90 [broad peaks, CH_2 backbone]. FT-IR [KBr, selected bands (cm^{-1})]: [3056, 3029, 3002, Ar−H]; [2946, 2867, CH, *ν* sym and antisym]; [758, 707, Ar−H, δ_{oop} o-disubstituted].

Poly(N,N-diallyl-N-methyl-N-(4-tert-butylbenzyl)ammonium) Chloride, ***4***. White hygroscopic powder. ^{1}H NMR (300 MHz, CD_3OD): δ = 7.80−7.35 [one signal, 4H, *Aromatic H*]; 4.80−4.20 [broad peak, ($^+$N)−CH_2−Φ], 4.10−2.20 [broad peaks, ($^+$N)−CH_3 + C−C−CH_2−(N^+)]; 1.11 [s, C−(CH_3)−Φ]; 1.80−0.90 [broad peaks, CH_2 backbone]. FT-IR [KBr, selected bands (cm^{-1})]: [3061, 3027, Ar−H stretching]; [2962, 2868, CH, *ν* sym and antisym]; [1394, 1366, (−C(CH_3)$_3$) bending]; 1114 [-O−SO_3^-, *ν*]; [841, Ar−H, o-disubstituted]; [619, −O−SO_3^-]; [554, Ar−H, para-disubstituted].

Synthesis of Copolymer ***9***. White hygroscopic powder. ^{1}H NMR (300 MHz, CD_3OD): δ = 7.90 [one signal, 4H, *Aromatic H*]; 7.32 [one signal, *Aromatic H*]; 5.2−4.6 [broad, ($^+$N)−CH_2−Φ]; 4.40−2.20 [broad peaks, ($^+$N)−CH_3 + C−C−CH_2−(N^+)]; 1.80−1.00 [broad peaks, CH_2 backbone]. FT-IR [KBr, selected bands (cm^{-1})]: [3093, 3030, 3005, Ar−H]; [2937, 2868, CH, *ν* sym and antisym]; [2231, −CN stretching, *ν*]; [1117, −O−SO_3^-]; [831, 756, Ar−H, δ_{oop} o-disubstituted]; [619, −O−SO_3^-, *ν*]; [554, Ar−H, o-disubstituted].

Results and Discussion

Synthesis of Monomers and Polymerization. Monomers **m2**−**m4** were prepared according to the synthetic route presented in Figure 2. The first step entails the preparation of the methydiallylamine obtained according to the Eschweiler−Clark methylation.[16−17] The second step arises on the quaternization reactions of the tertiary amine and was performed by reacting the amine with various benzyl halide residue. Though polymerizations were effected in aqueous solution in the

(17) Icke, R. N.; Wisegarver, B. B. *Org. Synth.* **1945,** *25*, 89.

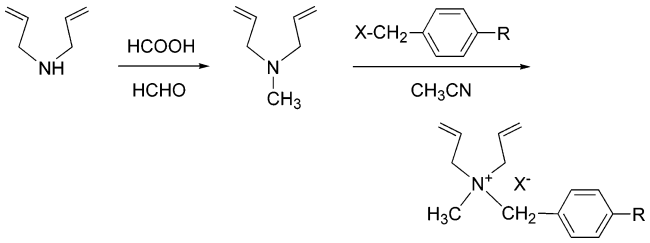

Figure 2. Synthetic route to monomers **m2**−**m4**.

presence of high amounts of initiator, the polymers were always obtained in low yields, i.e., typically less than 25% (w/w). No residual monomers could be detected after purification in the FT-IR or ^{1}H NMR spectra, judged by the absence of the typical signals of allylic moieties. As already put forward in a previous communication,[12] monomers seem to give low molar mass polymers only, as suggested by infrared bands at around 619−624 and 1114−1121 cm^{-1}. These are attributed to the vibrations of sulfate/sulfonate residues deriving from the initiator. Copolymerization leading to **9** was conducted in water with an equimolar amount of the two monomers, using $K_2S_2O_8$ as initiator. The chemical composition of the copolymer was determined by ^{1}H NMR spectra, by comparing the integration of the aromatic protons signals.

Thermal Properties. The thermal stability was investigated by thermogravimetric analysis with the aim to guarantee safe handling of the polyelectrolytes particularly at the time of the film fabrication. All polycations present a major degradation step occurring at around 365 °C and minor decomposition steps appearing at lower temperature and which are sensitive to the details of the chemical architecture. The onset of the first significant weight loss lies in the range of temperatures 130−175 °C according to the details of the chemical architecture. The limited thermogravimetric stability of the spiro compounds **7**[10,18] and **8**[12] were discussed before. The thermal decomposition temperatures of polycations **2** and **3** are observed at higher temperature, namely at around 170 °C.

Build-Up of Multilayered Films. To examine whether hydrophobized and sterically hindered water-soluble polyelectrolytes are still able to self-assemble regularly with Laponite (**L**), UV−Vis spectroscopy was employed using quartz substrates. Because maxima could not be determined easily from the absorbance spectra (Figure 3), the first derivative of the absorbance spectra was employed for better characterizing the assemblies $\{\mathbf{3},\mathbf{L}\}_n$, $\{\mathbf{8},\mathbf{L}\}_n$, and $\{\mathbf{9},\mathbf{L}\}_n$. Maxima of the peak corresponding to the $\pi \rightarrow \pi^*$ transitions of the benzyl fragment were evidenced around 200 and 220 nm for the $\{\mathbf{3},\mathbf{L}\}_n$ and $\{\mathbf{8},\mathbf{L}\}_n$ systems and at 202, 235, and 242 nm for the $\{\mathbf{9},\mathbf{L}\}_n$ assembly. The latter also exhibits a secondary maximum which appears at higher wavelength at 287 nm due to the auxochromic effect of the benzonitrile chromophore. As illustrated in the insets of Figure 3, the monotonic and linear increase in intensity for a given wavelength with the number of cycles suggests a regular adsorption of the two heterospecies. This confirms previous observations that the formation of hybrid assemblies from hydrophobized polycations with Laponite proceeds without particular problems.[7,10,12]

To better understand the effect on film growth of the specific nature of the substituents on the poly(diallylammonium) backbone, polycations were self-assembled with Laponite on silicon wafers, and the thickness of the films was determined by ellipsometry. The increase in the average thickness as a function of dipping cycle is presented in Figure 4. The figure illustrates well the linear sequential buildup of the two heterospecies when adsorbed from water or water/EtOH mixture or even from $CHCl_3$, regardless of the chemical nature of the polycation. The same trend was observed for DMSO based systems, too, namely for polycations **5** and **6**, but with less regularity possibly because of the photoreticulation or a desorption process.[12] These results confirm the general usefulness of poly(diallylammonium) derivatives for fabricating hybrid ESA assemblies, even those bearing large hydrophobic or bulky residues.

Still, these experiments reveal that the average thickness of the films depends significantly on the specific chemical structure of the polycations. This is also true for the solvents employed. Average thickness increments per cycle of deposition are given in Table 1.

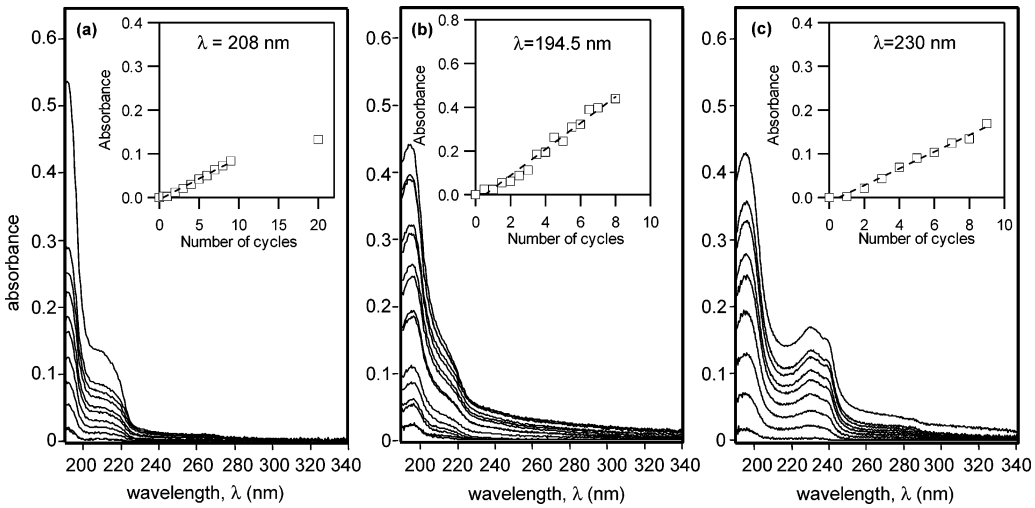

Figure 3. UV−Vis absorbance spectra of assemblies: (a) $\{\mathbf{3},\mathbf{L}\}_n$ (from bottom to top: n = 1, 2, 3, 4, 5, 7, 9, 20); (b) $\{\mathbf{8},\mathbf{L}\}_n$ (from bottom to top: n = 0.5, 1, 1.5, 2, 2.5, 3, 3.5, 4, 4.5, 5, 5.5, 6, 6.5, 7, 7.5, 8, 8.5, 9); (c) $\{\mathbf{9},\mathbf{L}\}_n$ (from bottom to top: n = 1, 2, 3, 4, 5, 6, 7, 8, 9) grown on quartz supports. Insets: relation between absorbance and number of cycles measured in the absorbance spectra at (a) 208 nm, (b) at 194.5 nm, and (c) at 230 nm.

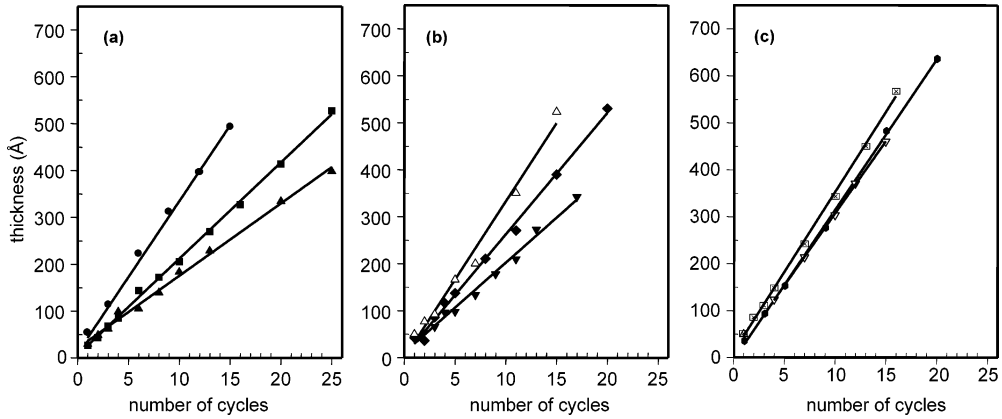

Figure 4. Evolution of ellipsometric thickness of layer-by-layer assembled films from Laponite **L** and various poly(diallylammonium salts). (a) Polycations with increasing bulkiness and rigidity due to the number of rings condensed to the polymer backbone: (▲) = {**1**,**L**}$_n$, (■) = {**7**,**L**}$_n$, (●) = {**8**,**L**}$_n$; (b) polycations with increasing hydrophilic−hydrophobic balance, due to the character of the substituents on the benzyl ring: (▼) = {**4**,**L**}$_n$, (■) = {**3**,**L**}$_n$, (△) {**2**,**L**}$_n$; (c) polycations with complex functional substituents: (▽) = {**9**,**L**}$_n$, (⬢) = {**10**,**L**}$_n$, (⊠) = {**11**,**L**}$_n$. Filled symbols: water-based systems. Open symbols: H_2O/EtOH based system. Square ×-hair: $CHCl_3$ based system.

For instance, the effect of bulkiness is illustrated in Figure 4a by the significant increase in the average thickness per adsorption cycle in the series of water-soluble polycations of increasing bulkiness **1**, **7**, and **8**. At present, one may only speculate on the reasons. On one hand, a more expanded conformation of the sterically more hindered polyelectrolyte **8** may account for the thicker layers. On the other hand, the increasing hydrophobic character of the substitutents may contribute to the increased thickness. The effect of hydrophobicity is clearly evidenced in Figure 4b. Film thickness increases in the order {**2**,**L**}$_n$ < {**3**,**L**}$_n$ < {**4**,**L**}$_n$, i.e., with increasing hydrophobicity of the substituents of the benzyl residue. A similar observation concerning the effect of hydrophobic fragments was reported for polymethacrylates in smectite−polyelectrolyte films.[10] Also, increasing thickness with increasing hydrophobic substitution of one of the polyions, was reported for ESA films made exclusively from flexible organic polyions.[19]

In agreement with the discussion above, substitution of the parent polycation **1** by more complex hydrophobic substituents, such as in multilayer films {**9**,**L**}$_n$, {**10**,**L**}$_n$, and {**11**,**L**}$_n$, results in increased film thicknesses (Figure 4c). Apparently, if the bulky hydrophobic pendent group is connected to the backbone by a flexible spacer, the increase in film thickness is limited, possibly due to the higher compliance of the side group. However, a more detailed analysis of the values is precluded by the necessary use of organic solvents for film deposition, which is known to influence film thickness, too.[1]

The structure formation in hybrid ESA films assembled on silicon wafers was investigated by XRR. Some representative X-ray reflectograms are shown in Figure 5a. The structural information obtained is consistent with that of previous communications.[10] Broad Bragg peaks are observed in each cases, irrespective of the detailed nature of the polycation employed and of the solvent used for building up the assembly, indicating the general presence of a lamellar structure of low coherence in such hybrid films. This demonstrates that

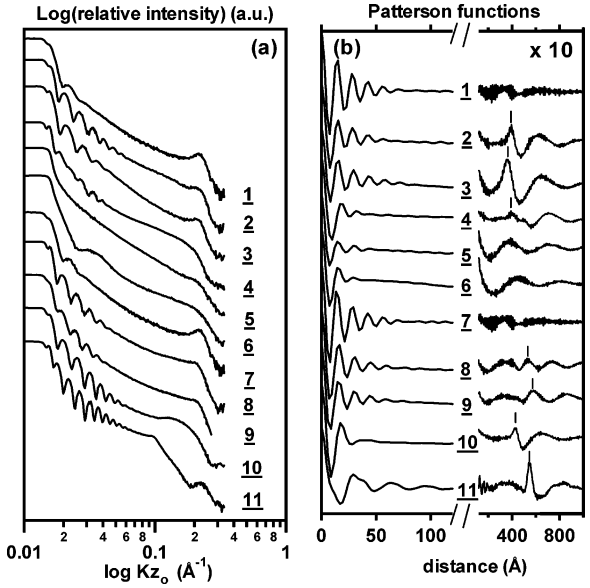

Figure 5. Structural data of {**A**,**L**}$_n$ hybrid multilayers. (a) X-ray reflectograms. From top to bottom: {**1**,**L**}$_{16}$, {**2**,**L**}$_{15}$, {**3**,**L**}$_{15}$, {**4**,**L**}$_{15}$, {**5**,**L**}$_{15}$, {**6**,**L**}$_{15}$, {**7**,**L**}$_{16}$, {**8**,**L**}$_{15}$, {**9**,**L**}$_{15}$, {**10**,**L**}$_{15}$, and {**11**,**L**}$_{16}$. Note the log−log scale. Curves are displaced vertically for clarity. (b) Patterson functions computed from the reflectivity data are displaced vertically for clarity. The vertical line indicates the location of the peak due to correlation between both film interfaces.

the general system {**A**,**L**}$_n$ is remarkably robust for structure formation, contrasting markedly with systems based on mesomorphic ionomers and montmorillonite, or hydrotalcite, respectively, described elsewhere.[20−21] The internal order of the films is also clearly evidenced by the presence of oscillations in Patterson functions, as shown by the representative traces in Figure 5b. Exponential damping of the Patterson functions illustrates the limited extent of a coherent vertical stacking, as discussed extensively elsewhere.[11] Films may be represented for their most part as vertically disordered except close to the substrates.[7,9−11]

(18) De Vynck, V.; Goethals, E. J. *Macromol. Rapid Commun.* **1997**, *18*, 149.
(19) Cochin, D.; Laschewsky A. *Macromol. Chem. Phys.* **1999**, *200*, 609.
(20) Laschewsky, A.; Wischerhoff, E.; Kauranen, M.; Persoons, A. *Macromolecules* **1997**, *30*, 8304.
(21) Cochin, D.; Passmann, M.; Wilbert, G.; Zentel, R.; Wischerhoff, E.; Laschewsky, A. *Macromolecules* **1997**, *30*, 4775.

In addition to the occurrence of Bragg peaks, the position and the number of the Kiessig fringes typically displayed in the small-angle region of the X-ray reflectograms provide information on the total thickness and the roughness of the films. For a given number of adsorption cycles, the roughness was found to be significantly lower for assemblies containing aromatic moieties [{**2**,**L**}$_{15}$ − {**4**,**L**}$_{15}$, {**6**,**L**}$_{15}$, {**8**,**L**}$_{15}$, {**10**,**L**}$_{15}$ − {**11**,**L**}$_{16}$] as compared to such without {**1**,**L**}$_{16}$, and to films {**1**,**M**}$_{15}$ made from montmorillonite **M**.[9] For example, reflectograms of the films {**11**,**L**}$_{16}$ present up to at least 10 well-visible distinct fringes pointing out the low roughness of both interfaces. This is also evidenced in the Patterson functions from the presence of a rightmost sharp peak for the smoother films (Figure 5b). The position of this peak was found to coincide rather well with the total average thickness of the film as measured by ellipsometry, confirming the correctness of the index of refraction taken to interpret the ellipsometric data. The roughness of the multilayers (as evaluated by the number of Kiessig fringes in the reflectograms) does not appear to correlate well with the quality of the layering (as judged from the intensity and width of the Bragg peaks). This is logical, since true layering exists only close to the substrate, far from the outer surface of the film, as was demonstrated elsewhere.[11]

The detailed chemical structure of the flexible polyelectrolytes (**1**−**10**) affects the size of the ordered regions (or correlation lengths), these extending on a length scale varying roughly between 31 and 75 Å for films formed from 15 to 16 deposition cycles (Table 1). The increasing bulkiness and rigidity of the polycations within the series **1**, **7**, and **8** seem to have no significant impact on the values L_{coh} of the coherence lengths. By contrast, increasing the hydrophobic character of the polycation affects negatively the coherence lengths ($\leq$41 Å), as demonstrated by the values obtained for the polycations **4**−**6** and **10**.

For polymers without amphiphilic character, the detailed chemical structure affects moderately the position of the Bragg peak, confirming previous observations.[10] The Bragg spacing varies between 14.3 Å for {**3**,**L**}$_n$ to 15.5 Å for {**8**,**L**}$_n$, and 18.7 Å for {**10**,**L**}$_n$ to 19.6 Å for {**4**,**L**}$_n$ for assemblies built from water and water/ethanol based systems, respectively. Accordingly, the thickness of the organic sublayers p is between 5.1 and 10.4 Å (Table 1). Similarly, a significant increase in the interlamellar spacing was reported when $\alpha-\omega$ polyphosphate sheets must accommodate bulky labeled polycations,[22] or when Laponite platelets intercalate poly(methacrylate)s with various side-chain length.[10] Nevertheless, it is not clear from the present data to which extent the variations of thickness may result from the choice of the solvent. Indeed, although significant, the dependence of the basal spacing with the molecular structure appears not very clearly within the series of films obtained from the systems based on same solvents.

Sample {**11**,**L**}$_n$ presents two Bragg reflections whose origins are not yet fully elucidated yet. Presumably, the mesogenic character of the cyano-bi-phenyl side group of polycation **11** is responsible for an increased degree of organization near the surface of the substrate, resulting in two levels of organization appearing in the sample.

The increment of thickness per adsorption cycle was also found to depend on the nature of the polycation. As a result, the ratio R (increment of thickness per adsorption cycle/Bragg spacing) is rarely equal to or close to one, and was found to vary between 0.3 and 2.1, depending on the nature of the polycation (see Table 1). This observation agrees well with what was found for other ordered {**A**,**B**}$_n$ multilayers.[2,6,10] It confirms that film growth cannot be explained by the simple alternate deposition of monolayers of platelets and polycation, as demonstrated for other systems,[23] but the primarily adsorbed polyelectrolytes may be subject to reorganization processes upon complexation, leading to internal structure in the thin films.[2,10]

Conclusions

Hybrid multilayers can be prepared by combining a wide variety of functional poly(diallylammonium) salts and Laponite through an alternating electrostatic self-assembly process. Bulky, hydrophobic, or even amphiphilic, residues can be intercalated between discrete aluminosilicates platelets obtained from disordered exfoliated synthetic clays. Such fragments can be incorporated without disrupting the lamellar-like lattice which prevails only close to the substrate. Small variations of the polycation structure affect only slightly the internal ordering of the multilayers in terms of interlayer spacing and coherence length, with the exception of the polycation disposing of mesogenic fragments. By contrast, the average thickness increment depends on the details of chemical structure, pointing out the effect of the polycation conformation in solution and its probable aggregation state. These results also confirm previous ones, indicating a virtual decoupling between the increment of film growth and the Bragg spacing.[2a] Finally, although ESA assemblies based on sequential adsorption of heterospecies with both long range order and very smooth interfaces have not yet been achieved by this approach, such structural properties may be tailored to some extent by the use of the appropriate polyion.

Acknowledgment. We gratefully acknowledge A. Moussa for the invaluable help provided in ellipsometry. Discussions with J.-L. Habib-Jiwan were highly appreciated. Funding for this work was provided by the Belgian National Fund for Scientific Research, and by the DG Recherche Scientifique of the French Community of Belgium (Action de Recherche Concertée, convention 00/05-261). We are also indebted to M. Devillers for access to thermogravimetric analysis. We are also grateful to F. Rullens and M. Cuypers for their participation in the synthesis of the cyanobiphenyl and the coumarine derivatives.

CM021338Q

(22) Kim, H. N.; Keller, S. W.; Mallouk, T. E.; Schmitt, J.; Decher, G. *Chem. Mater.* **1997**, *9*, 1414.

(23) Keller, S. W.; Wilson, W. L.; Johnson, S. A.; Brigham, E. S.; Yonemoto, E. H.; Mallouk, T. E. *J. Am. Chem. Soc.* **1995**, *117*, 12879.